Lab on a Chip

Cite this: *Lab Chip*, 2012, **12**, 2803–2806

www.rsc.org/loc

TECHNICAL INNOVATION

Microfluidic very large scale integration (mVLSI) with integrated micromechanical valves†

Ismail Emre Araci and Stephen R. Quake

Received 13th March 2012, Accepted 30th April 2012
DOI: 10.1039/c2lc40258k

Microfluidic chips with a high density of control elements are required to improve device performance parameters, such as throughput, sensitivity and dynamic range. In order to realize robust and accessible high-density microfluidic chips, we have fabricated a monolithic PDMS valve architecture with three layers, replacing the commonly used two-layer design. The design is realized through multi-layer soft lithography techniques, making it low cost and easy to fabricate. By carefully determining the process conditions of PDMS, we have demonstrated that 8 × 8 and 6 × 6 μm^2 valve sizes can be operated at around 180 and 280 kPa differential pressure, respectively. We have shown that these valves can be fabricated at densities approaching 1 million valves per cm^2, substantially exceeding the current state of the art of microfluidic large-scale integration (mLSI) (thousands of valves per cm^2). Because the density increase is greater than two orders of magnitude, we describe this technology as microfluidic very large scale integration (mVLSI), analogous to its electronic counterpart. We have captured and tracked fluorescent beads, and changed the electrical resistance of a fluidic channel by using these miniaturized valves in two different experiments, demonstrating that the valves are leakproof. We have also demonstrated that these valves can be addressed through multiplexing.

Introduction

Microfluidics is the science of systems that manipulate small amounts of fluids, generally on the nanoliter scale and below. Numerous applications of microfluidics have been developed for various fields such as chemistry and biology.[1–5] Additionally, many technological innovations have been developed to control fluid behaviour for these applications.[5–8] Amongst these, monolithic PDMS micromechanical valves[8] have been attractive due to ease of fabrication, low cost and scalability. The development of microfluidic chips with hundreds to thousands of integrated micromechanical valves is referred as microfluidic large scale integration (mLSI).[9,10]

mLSI enables hundreds to thousands of assays to be performed in parallel, using multiple reagents in an automated manner and has been used in applications such as protein crystallography,[11,12] genetic analysis,[1,2,13,14] high-throughput screening,[15] and chemical synthesis.[4]

There are two basic requirements for mLSI technology: monolithic microvalves that are leakproof and scalable, and a method of multiplexed addressing and control of these valves.[9,10] Typical valve dimension in mLSI studies reported so far are 100 μm or higher. Reducing the valve dimensions by an order of magnitude will enable chips with two orders of magnitude higher density. There have been recent demonstrations of high-density devices with limited functionality, mostly in the context of digital polymerase chain reaction (dPCR).[16–18] In a recent study, Heyries *et al.* demonstrated that one million chambers can be fabricated on a single chip (440k chambers per cm^2). This device does not have valves for external control but achieves a dynamic range of 10^7, single-nucleotide-variant detection below one copy per 100 000 wild-type sequences and the discrimination of a 1% difference in chromosome copy number. In dPCR, parallel screening of different mutations in a single experiment can significantly reduce the analysis time.[17] Pekin *et al.* demonstrated that 6 common KRAS mutations can be screened with droplet based dPCR. These are useful applications of density improvement but these are limited to simple manipulations. In order to solve the macroscopic–microfluidic interface problem for highly parallel analysis (>100 different experiments) on a single chip, control elements (*i.e.* valves) are required.[19] It is possible to achieve one million control elements in a single chip for micromechanical valve dimensions below 10 × 10 μm. This would allow automated control through utilizing techniques like on-chip multiplexing and on-chip reagent mixing[19] and provide high sensitivity and dynamic range, simultaneously.

In this manuscript we have developed a three-layer chip design in order to overcome reliability issues, which we have encountered during our miniaturization efforts of the two layer

Dept. of Bioengineering, Stanford University, and Howard Hughes Medical Institute, Stanford, CA 94305, USA.
E-mail: earaci@stanford.edu; Fax: (+650) 724-7383;
Tel: (+650) 724-5473

† Electronic supplementary information (ESI) available: Supplementary movies 1 and 2 are provided. See DOI: 10.1039/c2lc40258k

chip architecture. There are two different standard valve types, both with two-layer cross-section; push-up and push-down.[20] It has been shown previously that push-up type valves have lower actuation pressure compared to push-down valves due to flat geometry of the valve membrane. However, for both of these standard valve types, PDMS is spin coated on a mold which has photo-patterned resist features defining the chip design. Achieving a uniform membrane with a thickness much smaller than the resist thickness is not possible because of this spin-coating process made directly on the mold. In our proposed design a thin (<1 μm) PDMS film is sandwiched between flow and control layers as shown in Fig. 1a, providing a flat and uniform valve membrane similar to push-up valve geometry. Our design enabled us to make a size reduction of more than an order of magnitude (100 × 100 μm^2 to 6 × 6 μm^2) over standard monolithic micromechanical valves. We have reliably used the chips made by this technique over several days without any delamination or collapse. We have demonstrated that these valves are leakproof, can be multiplexed, and also that they can be made in more than two orders of magnitude higher densities than the mLSI (0.4M–0.8M valves/cm^2). We refer to this high density chip fabrication technique as microfluidic very large scale integration (mVLSI) analogous to electronic counterpart. This technology can also open new possibilities for the field of optofluidics since it pushes the scale of microfluidics one step closer to the scale of optical wavelengths.[21]

Design and fabrication

The thin valve membrane shown in Fig. 1a is obtained by spin coating PDMS on a blank silicon wafer at very high speeds and extended spin durations. This results in highly uniform films with a thickness as small as 0.3 μm. In our experiments we have also observed that as the PDMS cross-linker mixing ratio reduced from 1 : 10 to 1 : 30, the resulting film thickness reduced from 1 μm to 0.3 μm for a spin speed of 12 000 rpm, and spin duration of 15 min. Due to its low viscosity and low Young's modulus (E), PDMS with low cross-linker ratio (1 : 30) is used for the fabrication of valve membranes. In order to estimate the required membrane thickness range, we used the analytical model for circular membranes provided in literature.[22] According to this model, a thin film with a diameter $2a$ and thickness t, will require pressure,

$$P = \frac{C_1 t}{a^2}\sigma_0 w_0 + \frac{C_2 f(v) t}{a^4}\frac{E}{1-v}w_0^3 \quad (1)$$

in order to achieve a maximum deflection, w_0, at the centre of the membrane. Here v is the Poisson's ratio, σ_0 is the residual stress, C_1, C_2 and $f(v)$ are used as in Ref. 22 for circular membranes.

Fig. 1b shows the 3-dimensional surface plot of calculated pressure values required to obtain 3 μm deflection at the membrane center, with respect to membrane diameter and Young's modulus. The inlet shows the model geometry and description of the parameters. The thickness of the film in this calculation is taken as 0.3 μm. It is seen in the figure that, when membrane diameter is larger than 6 μm the required pressure is well below 280 kPa (a practical constraint, shown as a red line in Fig. 1b), for a large range of Young's modulus values. However,

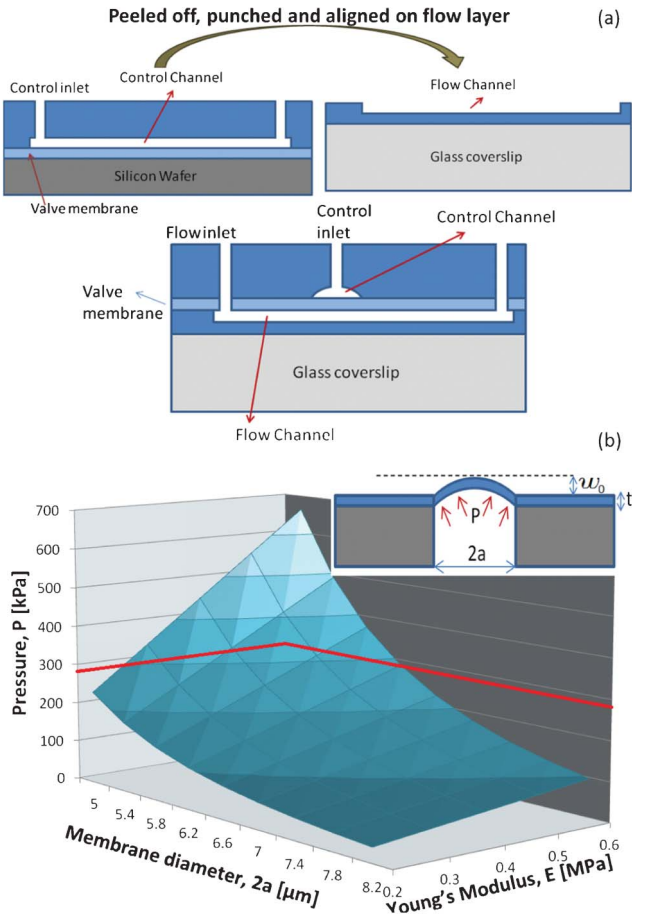

Fig. 1 (a) Intermediate fabrication steps (top) and cross section (bottom) of the three-layer design for microfluidic very large scale integration. (b) Required pressure to achieve 3 μm deflection, w_0, with respect to membrane diameter, $2a$ and Young's modulus, E, for membrane thickness t = 0.3 μm. The red line indicates the 280 kPa pressure value which can be practically applied to microfluidic chips. See the inlet for the schematics of the model geometry and description of the parameters.

for membranes with less than 6 μm diameter the Young's modulus constraint is much stricter.

Equipped with this information, we fabricated chips which have 4096 valves with different sizes (5, 6 and 8 μm) at high density (0.4–1 million valves per cm^2). We first prepared the control and flow molds by using standard lithography techniques described elsewhere.[20] The channel height was selected as 1.5 μm in order to ensure complete sealing of the valves at 3 μm maximum deflection. We used a 3′′ silicon wafer as a substrate for the valve membrane. Then we silanized the mold surfaces with tetramethylchrolosilane vapor for at least 2 h. PDMS (RTV615) mixture with a cross-linker ratio of 1 : 30 and volume of 1 mL was dropped on to the substrate and spin coated for 15 min at 12 000 rpm with a Laurell WS-650Mz-23NPP spin coater, and baked at 80 °C for 40 min. In the meantime, another PDMS (1 : 5) mixture was prepared for flow and control layers. PDMS was poured onto the control mold, degassed for 30 min and baked at 80 °C for 40 min. After this, PDMS for the control layer was cut, control channel access holes were punched and this layer was placed on to the valve membrane layer as shown in

Fig. 1a, top left. These two layers were baked in an 80 °C oven for 1.5 h for thermal bonding. After thermal bonding we waited for 10 min to let the sample cool down, and then peeled off both layers and punched access holes for flow channels. Flow layer was prepared as follows: PDMS was spin coated on the flow mold at 500 rpm for 1 min, which resulted in around 100 μm flow layer thickness. We placed the flow layer on a flat surface for 10 min and let any air bubbles disappear. The flow layer was then baked at 80 °C for 2 h. At the end of the baking process, the PDMS was cut and placed on a thin coverslip so that the patterned side was facing upwards, as shown in Fig. 1a, top right. The flow layer and the control/membrane layer were then bonded by plasma treatment technique; both layer surfaces were treated with O_2 plasma at 70 Watt and 0.2 mBar for 30 s. We used a manual X-Y-Z-stage from Newport, a manual homemade θ-stage and an OPTEM 125C imaging system, equipped with a 10× long working distance objective and a CCD camera for alignment. The flow layer was fixed on the θ-stage and the control layer was placed on a thin glass coverslip to minimize optical aberrations, which was held by a vacuum chuck and subsequently placed on the X-Y-Z stage. The two layers were aligned within 2 micron precision and brought into contact for bonding. We believe motorized stages can be used for better precision. The chip was finally baked for another 10 min in order to ensure a stronger bond between control/membrane and flow layers. We then tested the chips.

Characterization

Fig. 2 shows the 8 and 6 μm valves before (open) and after (closed) actuation at 280 kPa. We have successfully controlled all the valves simultaneously for the 6 and 8 μm valve size (see Supplementary movie 1†). Although some of the 5 μm valves were functional, the results were less consistent. The lateral shrinkage of the valves due to deformation of PDMS under the applied control line pressure was 1 μm for both channel sizes.

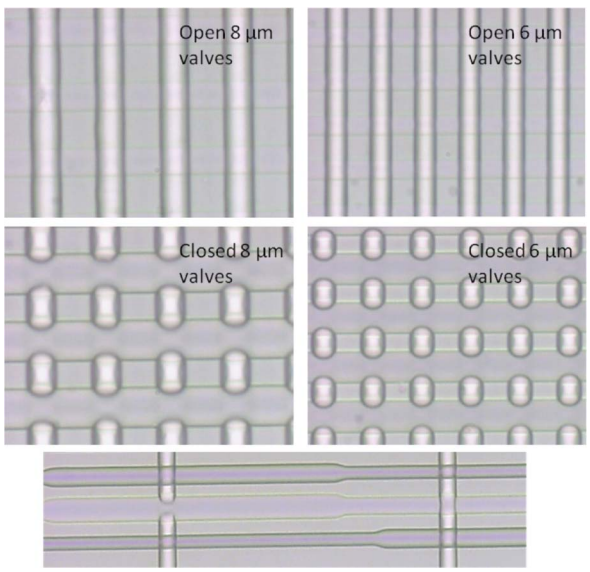

Fig. 2 Open (top) and closed (middle) 8 × 8 and 6 × 6 μm^2 valves under differential pressure ($P_{control} - P_{flow}$) of 280 kPa. Demonstration of the channel crossover (bottom); the flow channel on the left is closed while the one on the right remains open when the control channel width is reduced to 4 μm or less.

We have operated the 8 μm valves at 5 Hz. This value is about an order of magnitude lower than standard valves.[8] The temporal response of miniaturized valves is mainly due to their slow closing times. The two factors that contribute to the slow valve closing are: first, the applied force cannot be increased above 0.02 mN (50 times lower than typical force in standard valves) because of the small valve dimensions and second, the high spring force (>200 kPa) of the valves.

For microfluidic multiplexing, it is required to cross flow channels when desired.[9] We have observed that when the control channel dimension is 4 μm or less, it is possible to cross 6–8 μm wide flow channels without disturbing their flow, which demonstrates the multiplexing capability of miniaturized valves. The bottom image in Fig. 2 shows that 6 × 6 μm^2 valve on the left is closed and 3 × 6 μm^2 valve on the right is open.

After showing that 6 and 8 μm valves are scalable and can be multiplexed, we demonstrated that this valve architecture is leakproof by tracking the motion of 0.5 μm diameter fluorescent beads in 8 μm wide channels, which are controlled by the miniaturized valves. According to the well known one dimensional diffusion equation, average displacement-squared is given as;

$$<x^2> = 2Dt$$

where D [m^2 s^{-1}] is the diffusion constant and t [sec] is the diffusion time. The diffusion constant for a bead with 0.5 μm diameter in water is on the scale of 10^{-12} m^2 s^{-1}, which makes the expected displacement in 10 min duration about 100 μm. In order to demonstrate that the valves completely seal the flow channels, we first applied 35 kPa pressure to the flow channel and observed the movement of beads as shown in Fig. 3 top image. It is clearly seen that, when the beads are affected from the applied pressure, their fast drift motion results in a continuous fluorescence trace.

At $t = 0$ we closed both up and downstream valves and have trapped beads in a single channel. One of these trapped beads is shown in Fig. 3, middle left. We observed the motion of the bead for 10 min and at the end the bead was still within the diffusion distance as shown in Fig. 3, middle, right. We showed the track of the bead making Brownian motion for 5 min time period in Fig. 3 bottom image. The red and green dot shows the start and end location of the bead, respectively. It is seen that the pressure difference in the flow channel does not cause a net drift in the direction of the flow, which demonstrates that the valves are leakproof. We have also trapped a single 0.1 μm diameter fluorescent bead in a single 8 × 8 μm^2 chamber and recorded the bead movement for 5 min (see the Supplementary movie 2†).

Finally, we characterized the valve behaviour by using an experimental technique described elsewhere.[23] We filled the flow channels with $MgCl_2$ solution in water for standard and miniaturized valve architectures with dimensions of 100 × 100 × 8 and 8 × 8 × 1.5 μm, respectively. The electrical resistance along the fluidic channels was measured continuously as the differential pressure ($P_{control} - P_{flow}$) was increased and then decreased. Fig. 4 shows the hysteresis curves obtained from the measurement. The red line is for the miniaturized valves and blue is for standard push-down geometry. The resistance difference of

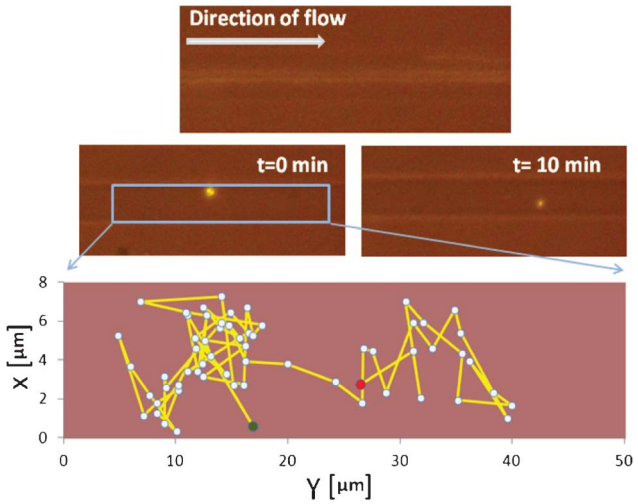

Fig. 3 Valve sealing is demonstrated by observing the Brownian motion of the beads; Top: 0.5 um diameter fluorescent beads are flowing in the direction of the white arrow under 35 kPa flow channel pressure, the fluorescence traces of flowing beads are visible. Middle: The up- and downstream valves of the flow channel are closed at 200 kPa differential pressure while the flow channel is still pressurized. A captured bead is shown at $t = 0$. After 10 min of free motion, the same bead is shown on middle, right. The photobleaching of the bead fluorescence signal is observed due to constant excitation. Bottom: The track of the bead for a 5 min period with 5 s. intervals is shown.

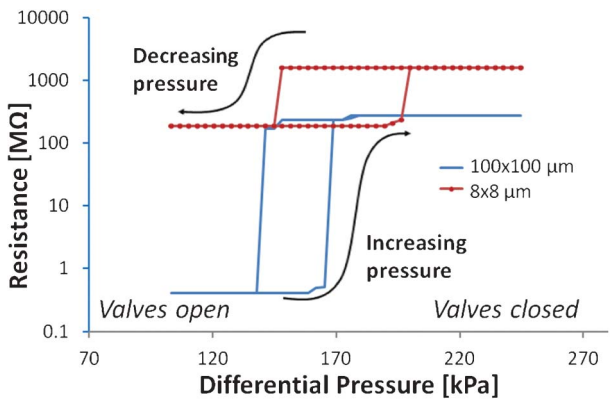

Fig. 4 Hysteresis curves showing the electrical resistance of a flow channel filled with $MgCl_2$ solution in water with respect to differential pressure applied to control channel. The blue curve is for 100 μm flow channel width and red curve is for 8 μm flow channel width.

the two valve types for the open valve state is consistent with the difference in channel size and length. When the valves are closed, the resistance of standard valves increased to around 200 MΩ (more than 2 orders of magnitude isolation is in agreement with Ref. 23) and the resistance of miniaturized valves exceeded 1 GΩ (maximum resistance which can be measured by our setup). The similar characteristic shapes of two different valve types can be interpreted as another indication for valve sealing. For 8 μm valves, the valve closure pressure is found at 190 kPa; however, after closing the valves they remain sealed even when the pressure is reduced down to 150 kPa.

Conclusions

We developed a technique for fabrication of leakproof and robust miniaturized valves. The valves are proven to be scalable, and addressable by multiplexing. We refer to this technique as mVLSI because it allows more than two orders of magnitude density improvement over mLSI. mVLSI is attractive for improving throughput, sensitivity and dynamic range in various chemical and biological applications. One million addressable chambers would make it is possible to configure a single chip for hundreds of different experiments, or one single experiment with much higher sensitivity and dynamic range. The mVLSI technology is also attractive to the field of optofluidics because the smaller channel size would allow easier integration with single mode photonics devices.[21] mVLSI is enabled by the proposed three-layer chip design and by rigorous selection of the PDMS processing conditions. We observed that both 6 and 8 μm valves can be fabricated and used over several days, reproducibly.

References

1 H. C. Fan, J. B. Wang, A. Potanina and S. R. Quake, *Nat. Biotechnol.*, 2011, **29**, 51–57.
2 Y. Taniguchi, P. J. Choi, G. W. Li, H. Y. Chen, M. Babu, J. Hearn, A. Emili and X. S. Xie, *Science*, 2010, **329**, 533–538.
3 S. K. Sia and G. M. Whitesides, *Electrophoresis*, 2003, **24**, 3563–3576.
4 A. J. deMello, *Nature*, 2006, **442**, 394–402.
5 W. H. Grover and R. A. Mathies, *Lab Chip*, 2005, **5**, 1033–1040.
6 D. B. Weibel, M. Kruithof, S. Potenta, S. K. Sia, A. Lee and G. M. Whitesides, *Anal. Chem.*, 2005, **77**, 4726–4733.
7 A. W. Martinez, S. T. Phillips and G. M. Whitesides, *Proc. Natl. Acad. Sci. U. S. A.*, 2008, **105**, 19606–19611.
8 M. A. Unger, H. P. Chou, T. Thorsen, A. Scherer and S. R. Quake, *Science*, 2000, **288**, 113–116.
9 T. Thorsen, S. J. Maerkl and S. R. Quake, *Science*, 2002, **298**, 580–584.
10 J. Melin and S. R. Quake, *Annu. Rev. Biophys. Biomol. Struct.*, 2007, **36**, 213–231.
11 L. Li and R. F. Ismagilov, *Annu. Rev. Biophys.*, 2010, **39**, 139–158.
12 M. J. Anderson, C. L. Hansen and S. R. Quake, *Biophys. J.*, 2005, **88**, 55a–55a.
13 C. Jensen, Y. Zeng, J. Kim and R. A. Mathies, *JALA*, 2010, **15**, 455–463.
14 R. H. Liu, J. N. Yang, R. Lenigk, J. Bonanno and P. Grodzinski, *Anal. Chem.*, 2004, **76**, 1824–1831.
15 C. B. Rohde, F. Zeng, R. Gonzalez-Rubio, M. Angel and M. F. Yanik, *Proc. Natl. Acad. Sci. U. S. A.*, 2007, **104**, 13891–13895.
16 K. A. Heyries, C. Tropini, M. VanInsberghe, C. Doolin, O. I. Petriv, A. Singhal, K. Leung, C. B. Hughesman and C. L. Hansen, *Nat. Methods*, 2011, **8**, 649-U664.
17 D. Pekin, Y. Skhiri, J. C. Baret, D. Le Corre, L. Mazutis, C. Ben Salem, F. Millot, A. El Harrak, J. B. Hutchison, J. W. Larson, D. R. Link, P. Laurent-Puig, A. D. Griffiths and V. Taly, *Lab Chip*, 2011, **11**, 2156–2166.
18 L. B. Pinheiro, V. A. Coleman, C. M. Hindson, J. Herrmann, B. J. Hindson, S. Bhat and K. R. Emslie, *Anal. Chem.*, 2012, **84**, 1003–1011.
19 J. Liu, C. Hansen and S. R. Quake, *Anal. Chem.*, 2003, **75**, 4718–4723.
20 V. Studer, G. Hang, A. Pandolfi, M. Ortiz, W. F. Anderson and S. R. Quake, *J. Appl. Phys.*, 2004, **95**, 393–398.
21 D. Psaltis, S. R. Quake and C. H. Yang, *Nature*, 2006, **442**, 381–386.
22 A. L. Thangawng, R. S. Ruoff, M. A. Swartz and M. R. Glucksberg, *Biomed. Microdevices*, 2007, **9**, 587–595.
23 H. Chen, W. Gu, N. Cellar, R. Kennedy, S. Takayama and J. C. Meiners, *Anal. Chem.*, 2008, **80**, 6110–6113.

